nature neuroscience

Spine growth precedes synapse formation in the adult neocortex *in vivo*

Graham W Knott[1,3], Anthony Holtmaat[2,3], Linda Wilbrecht[2], Egbert Welker[1] & Karel Svoboda[2]

Dendritic spines appear and disappear in an experience-dependent manner. Although some new spines have been shown to contain synapses, little is known about the relationship between spine addition and synapse formation, the relative time course of these events, or whether they are coupled to *de novo* growth of axonal boutons. We imaged dendrites in barrel cortex of adult mice over 1 month, tracking gains and losses of spines. Using serial section electron microscopy, we analyzed the ultrastructure of spines and associated boutons. Spines reconstructed shortly after they appeared often lacked synapses, whereas spines that persisted for 4 d or more always had synapses. New spines had a large surface-to-volume ratio and preferentially contacted boutons with other synapses. In some instances, two new spines contacted the same axon. Our data show that spine growth precedes synapse formation and that new synapses form preferentially onto existing boutons.

Most excitatory synapses in the cerebral cortex terminate on dendritic spines[1]. Spines are structurally heterogeneous, varying in volumes by more than a factor of 100. Spine volumes are proportional to the area of the postsynaptic density (PSD)[2], AMPA receptor (AMPAR) content[3–5], and the size of the presynapse[2], suggesting that spine size is directly related to synaptic strength.

Recent work has focused on dendritic spines as a possible substrate of circuit plasticity in the adult brain. Neural circuits are sculpted by spontaneous activity and sensory experience[6]. Functional rewiring in the adult brain may involve structural plasticity with synapse formation and elimination[7–12]. Long-term *in vivo* imaging in the neocortex has revealed that a subpopulation of spines appear and disappear, whereas other spines persist for months[10,13,14]. In the barrel cortex, the lifetime of dendritic spines can be modulated by changes in sensory experience by whisker trimming[10,15,16].

How does spine addition relate to synapse formation? In cultured preparations, spines can emerge in response to synaptic stimulation[17,18] associated with synapse formation[19]. *In vivo* imaging experiments followed by electron microscopy have revealed that some new spines are associated with synapses[10]. However, these experiments did not distinguish whether new spines grow from previously existing shaft synapses (Miller-Peters model)[20–22] or whether new spines grow to contact a local axon with *de novo* synapse formation (Filopodia model)[23]. It is also unclear whether new spines form synapses on new boutons or preferentially contact existing boutons[8,12,20].

Here we reconstructed imaged dendritic spines and the surrounding neuropil using serial section electron microscopy (ssEM). New spines that persisted for a few days always had synapses. An analysis of the connectivity and geometry of axons and dendrites in the vicinity of new spines revealed that spine growth is followed by synapse formation. New spines preferentially formed synapses on multisynapse boutons, indicating that synapse formation does not correspond in a one-to-one fashion to the addition of axonal boutons.

RESULTS

We imaged dendrites in layer (L) 1 of transgenic mice expressing enhanced green fluorescent protein (EGFP) in a sparse subset of pyramidal neurons (line GFP-M)[24]. Two-photon laser-scanning microscopy[25] allowed long-term, high-resolution imaging through a cranial window placed over the barrel cortex[10,14] (**Fig. 1a**,**b**). Dendrites and their spines were imaged every 4 d for at least 28 d. Chessboard whisker trimming was initiated immediately after the third imaging session and lasted until the end of the experiment, at least 20 d. Clear cases of spine gains and losses were scored. Consistent with previous experiments, a subpopulation of spines appeared and disappeared from one imaging session to the next[14,16]. A fraction of these new spines (~10%) survived for more than 1 week and until the end of the imaging experiment (new persistent spines; for details on the *in vivo* imaging experiment see ref. 16).

Ultrastructural analysis of imaged dendritic spines

At the end of the *in vivo* imaging experiments, mice that had experienced whisker trimming ($n = 4$; one neuron per mouse) were processed for ssEM. The mice were fixed on experimental days 28 ($n = 2$), 29 ($n = 1$) and 30 ($n = 1$); therefore, two mice were imaged one additional time with a smaller time interval (1 and 2 d, respectively). Thick (60 μm) sections were cut, parallel to the optical plane of the *in vivo* images. Dendrites were stained for electron microscopy using pre-embedding immunohistochemistry for GFP. Individual sections were compared to projections of *in vivo* image stacks (**Fig. 1b**,**c**) to

[1]Département de Biologie Cellulaire et de Morphologie, University of Lausanne, Lausanne CH1005, Switzerland. [2]Howard Hughes Medical Institute, Cold Spring Harbor Laboratory, Cold Spring Harbor, New York 11724, USA. [3]These authors contributed equally to this work. Correspondence should be addressed to G.K. (Graham.Knott@unil.ch).

Received 24 March; accepted 14 July; published online 6 August 2006; doi:10.1038/nn1747

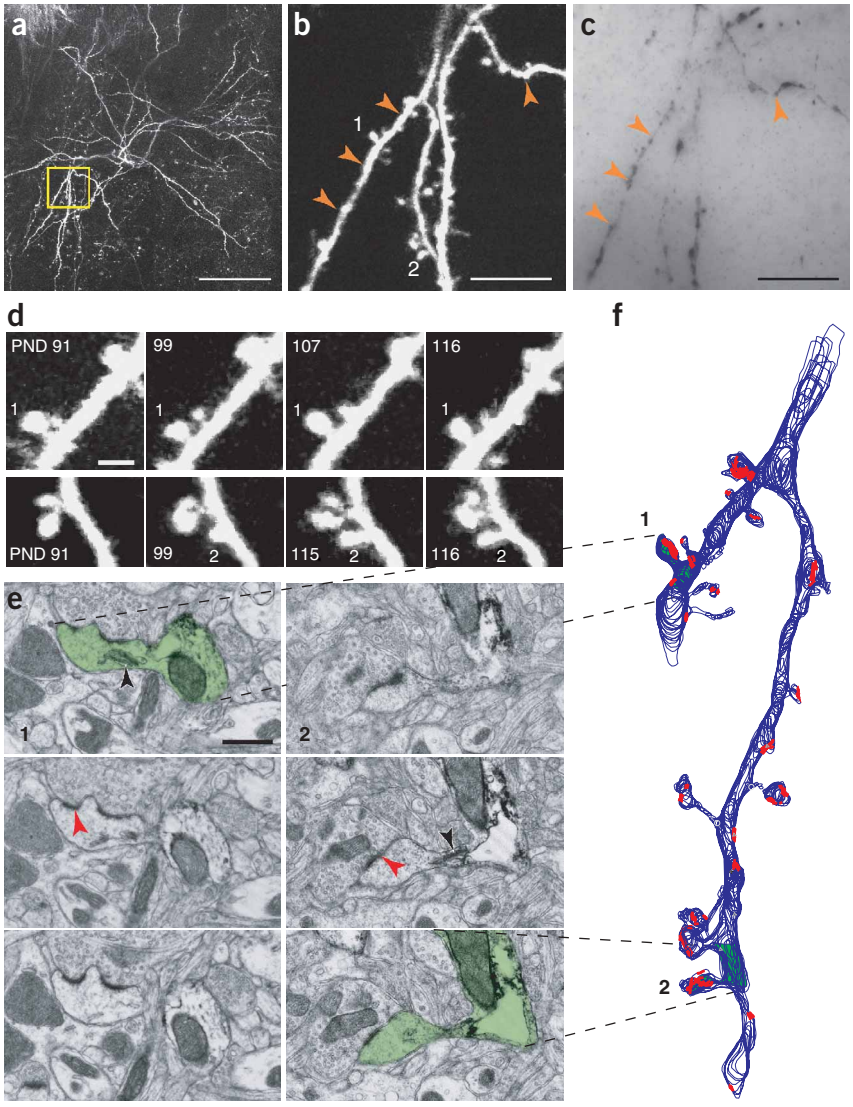

Figure 1 High-resolution *in vivo* imaging and retrospective serial section electron microscopy. (**a**) *In vivo* image of the apical dendritic tuft (top view) of a GFP-expressing layer 5B pyramidal neuron in the barrel cortex. (**b**) *In vivo* image of the boxed region in **a**, taken just before fixation. (**c**) A 60-μm-thick resin section after immunocytochemistry, before serial sectioning and EM. Dendrites in this figure correspond to orange arrowheads in **b**. (**d**) Time-lapse images showing a spine ('1') that persists throughout the experiment (upper series) and spine addition ('2', lower series) from the dendritic branches shown in **b**, and in the boxed region in **a**. (**e**) Serial electron micrographs through spines 1 (left-hand series) and 2 (right-hand series). Each spine has a head with an asymmetric synapse (red arrowheads). One micrograph in each series has been pseudocolored to indicate the imaged dendritic spine. In both cases, the DAB labeling can be seen within the dendrite as well as in parts of the spine. Black arrowheads indicate the SER. (**f**) Part of the labeled dendrite in **b** reconstructed in 3D from serial electron micrographs. The drawing of the spines shown in **e** are indicated in green in the reconstruction. The asymmetric synapses are drawn in red. Scale bars: 100 μm in **a**; 10 μm in **b** and **c**; 2 μm in **d**; 0.5 μm in **e**.

locate dendritic segments of interest. Previously imaged dendritic branches were identified using the vascular pattern on the surface of the cortex and local structural features (for example, dendritic branch points and its overall form; orange arrowheads in **Fig. 1b**,**c**). Based on the time-lapse images, we selected regions of interest with new spines for ssEM analysis (**Fig. 1d**). Small blocks, cut from the thick sections, were serially sectioned at 60-nm thickness for viewing in the electron microscope. Each thin section that contained the dendrite of interest was then photographed in the electron microscope (**Fig. 1e**). The dendrite was subsequently reconstructed in three dimensions (3D; **Fig. 1f**). All spines seen in the two-photon image could be located along the dendrite in the EM reconstruction (**Fig. 1b**,**f**).

Our sample included dendritic segments from three L5B pyramidal cells, all with structurally complex apical tufts[16]. The fourth cell was a L2/3 pyramidal neuron. All segments were from approximately the same depth in L1 (~50 μm below the pia). A total of 300.6 μm of imaged dendrite, including 159 spines, were reconstructed (**Supplementary Fig. 1** online). L5B dendritic shafts showed variable diameters, ranging from 0.2 μm to 1.0 μm (ref. 26). L2/3 dendrites had a more homogeneous caliber (diameter ~ 0.6 μm).

Synapses were classified as asymmetric (n = 182), presumed glutamatergic, or symmetric (n = 17), presumed GABAergic, based on the thickness of the presynaptic density relative to that of the postsynaptic one. These criteria have previously been verified in L4 of the somatosensory cortex of the adult mouse[9]. Symmetric synapses were typically on shafts (15 of 17), whereas asymmetric synapses were mostly on spines (136 of 182).

From the imaged and reconstructed dendrites, we analyzed 57 dendritic spines (48 in L5B; 9 in L2/3) and their surrounding neuropil (**Supplementary Table 1** online). In the *in vivo* images, these spines could be clearly seen as dendritic protrusions (**Fig. 1d**). The density of spines was lower on L5B (0.45 μm^{-1}) than on L2/3 (0.83 μm^{-1}) dendrites[14]. Spines were either present throughout the experiment (>28 d; 24 'always-present' spines), or they were new (range of ages: 0–28 d, 33 spines). We did not find mitochondria in any dendritic spine[27]. In all cases the spines imaged *in vivo* were found in the ssEM reconstructions (**Fig. 1b**,**f**). Conversely, all protrusions emanating in the horizontal plane from the dendrite in the ssEM reconstructions were detected in our *in vivo* images. We also analyzed 25 asymmetric shaft synapses.

New persistent spines have synapses

We analyzed imaged spines for evidence of synapses. Spines were considered to have synapses if they had a PSD, and an active zone directly apposed to the PSD, within boutons containing synaptic vesicles (**Figs. 1e** and **2a**, and ref. 28). Next, we considered the histories of individual spines. All always-present spines (n = 24) had asymmetric synapses (**Fig. 2**; >28 d). Similarly, all new spines that were seen for more than one imaging session (n = 18) had asymmetric synapses (**Fig. 2a**,**b** and ref. 16). The ages of these spines ranged from 2 d to 28 d. Two symmetric synapses were found on new spines. The youngest group of spines, those that were first seen in the last imaging session of the experiment, often did not have synapses (13 of 19; **Fig. 2b**,

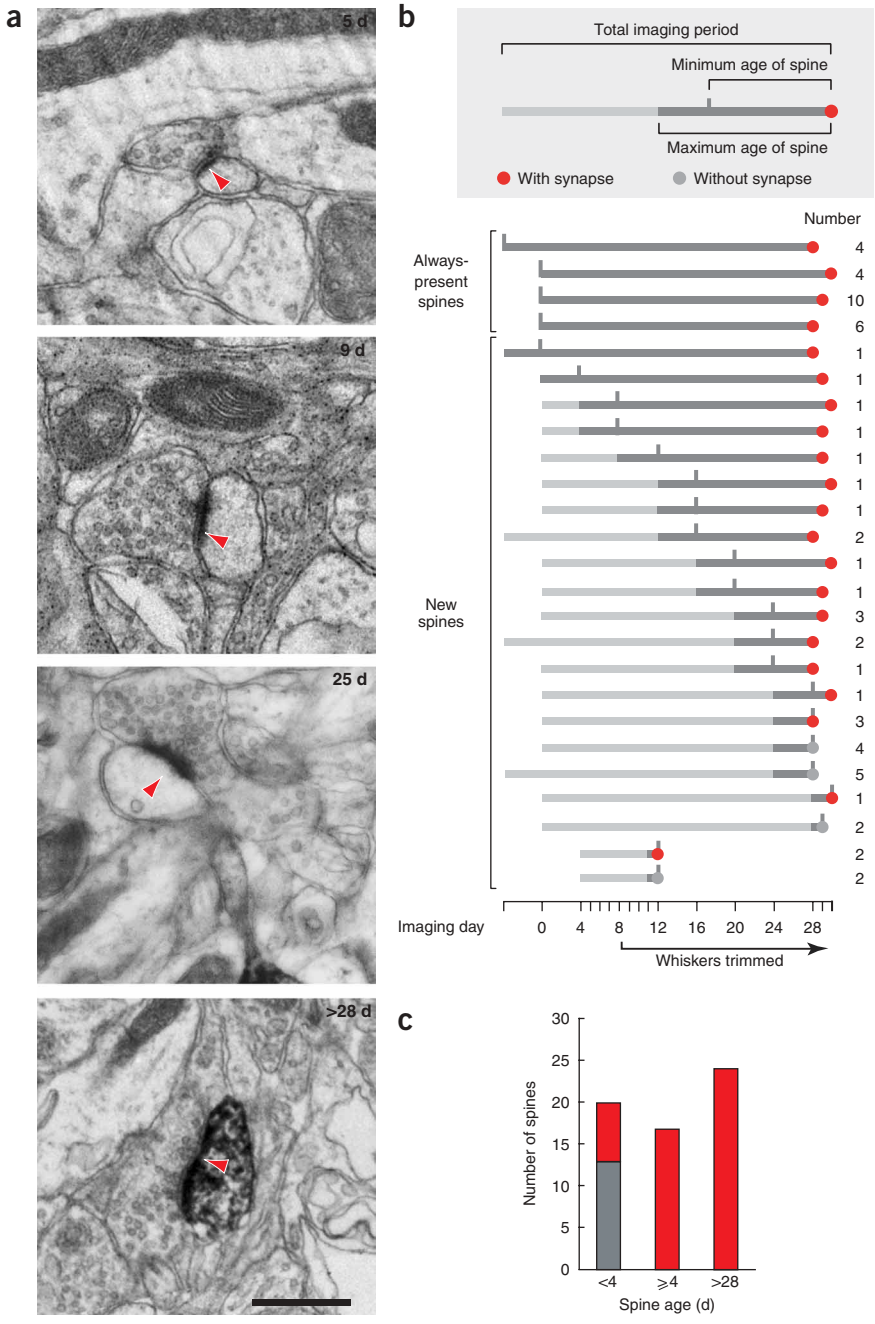

Figure 2 Synapses on new spines. (**a**) Electron micrographs showing synapses made by dendritic spines (red arrowheads); the minimum age of the spine is indicated in the top right corner. (**b**) Timelines of imaged spines that were analyzed with ssEM. Gray bars indicate the total imaging period. Ticks mark the time point at which spines were first seen. Dark gray bars define the maximum possible spine age. Circles at the end of the bars indicate the outcome of the ssEM analysis: red, with synapse; gray, without synapse. (**c**) The number of spines with (red) and without (gray) synapses that were less than 4 d old (first bar), 4–28 d old (second bar) and >28 d old (third bar). Panels **b** and **c** also include four new spines that were reconstructed as part of a previous study[10] (daily imaging for 8 d). Scale bar in **a**, 0.5 μm.

including 4 spines from ref. 10; **Supplementary Figs. 2** and **3** online). Because the interval between the last two imaging sessions was 4 d for most of these spines, their ages could range from 0 d to 4 d. We concluded that new spines, present for a few days or more, always have synapses, whereas the youngest spines often lack synapses (**Fig. 2b**,**c**).

Spine maturation

Time-lapse imaging studies have suggested that changes in spine structure may be associated with synapse formation or maturation[16,29]. New spines sometimes appeared as dim structures, indicating that they had small cytoplasmic volumes (**Fig. 3a** and ref. 14), and in later imaging sessions acquired a bright spine head (for example, spine 6 in **Fig. 3**; see also **Supplementary Fig. 3** and ref. 16).

To analyze the process of structural maturation in more detail, we measured spine volumes (V_{sp}), membrane surface areas (S_{sp}) and PSD areas (S_{PSD}) from the ssEM reconstructions. Spine volumes (V_{sp}) were distributed over a large range (L5B, 0.015–0.77 μm^3, **Fig. 3b** and **Supplementary Table 1**; L2/3, 0.018–0.15 μm^3). We found that L2/3 spines were more homogeneous than L5B spines. We therefore did not pool spines from the two cell types but focused on the larger group (L5B) for detailed structural analysis. New spines without synapses had smaller volumes and larger surface-to-volume ratios (S_{sp}/V_{sp}) than new spines with synapses ($P < 0.005$; **Fig. 3b**,**c**). In addition, new spines with synapses had larger S_{sp}/V_{sp} than always-present spines ($P < 0.005$). Therefore, spines form as relatively thin protrusions, add cytoplasmic volume as they form synapses, and continue to mature by adding volume. Because V_{sp} and S_{PSD} were highly correlated ($R = 0.84$; $P < 0.0001$; **Fig. 3d** and ref. 2), the decrease in S_{sp}/V_{sp} with spine age may reflect increasing synaptic strength.

We also analyzed spine shape based on criteria previously defined in the context of EM studies in the rat cortex[30] (**Supplementary Table 1**). Spines can be grouped into three different classes: thin, mushroom and stubby. Thin spines have lengths that are much larger than their diameters, and the diameters of their heads and necks are similar (in some studies thin spines have been called 'filopodia': refs. 13,15,31). Mushroom spines have head diameters that are much greater than their neck diameters. Stubby spines are short and have similar head and neck diameters. The majority of always-present spines were mushroom spines (mushroom 16 of 20, spines 8–10 in **Fig. 3**; thin 3 of 20; stubby 1 of 20). The new spines that were present for more than one imaging session were also mostly mushroom spines (mushroom 10 of 14, spines 5–7 in **Fig. 3**; thin 3 of 14, spines 3 and 4 in **Fig. 3**; stubby 1 of 14). In contrast, new spines seen only in the final imaging session (<4 d old) were mostly thin (mushroom 3 of 14; thin 11 of 14: for example, spines 1 and 2 in **Fig. 3**).

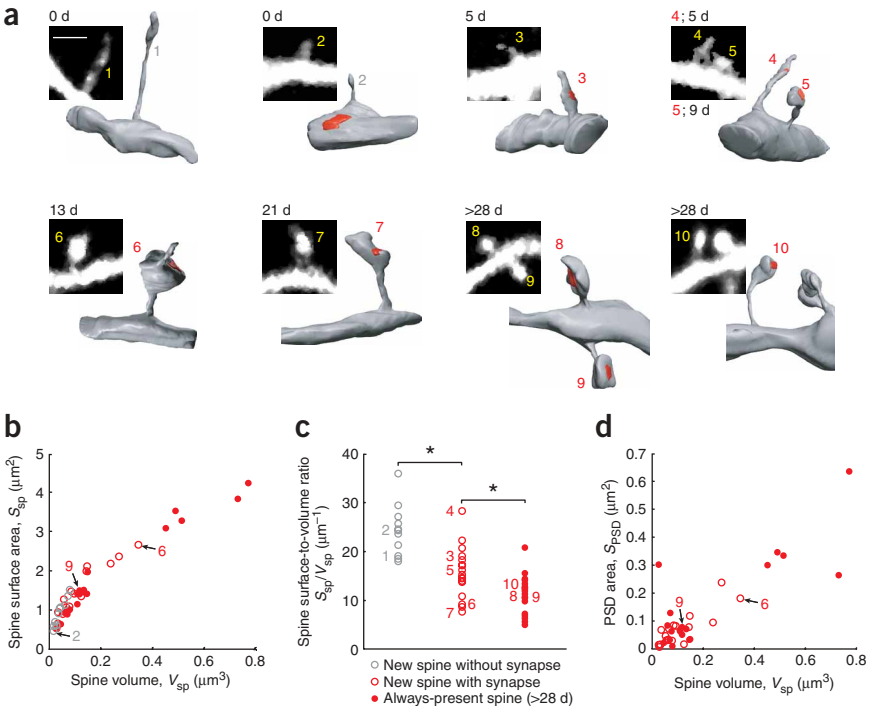

Figure 3 Morphometric analysis of new spines. (**a**) *In vivo* images of dendritic spines and the corresponding ssEM reconstructions. Synapses are shown in red. Minimum age of each spine is indicated. (**b**) Spine surface area (S_{sp}) plotted as a function of spine volume (V_{sp}; numbers refer to spines in **a**). (**c**) Distribution of spine surface-to-volume ratios (S_{sp}/V_{sp}) as a function of their age. All groups are significantly different ($^*P < 0.005$). (**d**) Spine PSD area (S_{PSD}) as a function of spine volume (V_{sp}). Spines 1, 6 and 7 are also shown in **Supplementary Figures 2** and **3** with their time-lapse images and three serial EM micrographs each. Scale bar in **a**, 2 μm; all other *in vivo* images are the same magnification.

In most of the reconstructed spines, the accumulation of the diaminobenzidine (DAB) reaction product was limited and did not obscure internal structures (24 of 24 always present; 28 of 33 new; including L2/3 spines). This allowed us to see whether the spines contained smooth endoplasmic reticulum (SER) or an organized spine apparatus, defined as stacked SER cisterns (black arrowheads in **Fig. 1e**, spines 1 and 3; **Supplementary Table 1** and refs. 32,33). Most (17 of 24) of the always-present spines contained either a well-defined spine apparatus or SER (**Fig. 1e**, spine 1). Only a few new spines (8 of 28) contained a small amount of SER, and all of these had synapses (**Fig. 1e**, spine 2). Of the new spines that were seen only once *in vivo* (<4 d old), only one spine had SER or spine apparatus. This suggests that SER and spine apparatus appear over several days after spine and synapse formation and may be associated with long-term maintenance of these structures.

Spine addition is associated with synapse formation

New spines and their target axons were embedded in a dense neuropil (**Figs. 1e** and **2a,** and **Supplementary Figs. 2** and **3**). The conversion of a shaft synapse to a spine synapse (Miller-Peters model of spinogenesis[21]) would require an axon to move laterally through the neuropil over 1 μm or more. To look for evidence of such movement, we analyzed stacks of EM images (3 × 3 × 3 μm³) containing new spines and their parent dendrites. The stacks included the presynaptic bouton, a short stretch of its axon, other axons and dendrites, and supporting cells.

Spines and their target axons were entangled with other axons and dendrites (**Fig. 4**). We found two instances where a pair of new spines made synapses with the same axon (**Fig. 4a**,**b**). Together with their parent dendrites, and target axons, these pairs of spines formed closed loops. Threaded through these loops were axons and dendrites (6 neurites in **Fig. 4a**, only 3 are drawn; 7 in **Fig. 4b**, only 1 is drawn), which traversed the entire sample volume. Because the large-scale structure of dendrites[10,34,35] and axons[36] is mostly stable in the adult brain, it is unlikely that all the neurites coursing between the new spines appeared after spine growth. In these cases, conversion of shaft-synapse to spine-synapse would require that the target axon crosses other neurites in the neuropil.

Further evidence against the Miller-Peters model comes from the analysis of boutons. New spines often made synapses on boutons that also contained synapses with other spines (multisynapse boutons, MSBs, 10 of 15), typically belonging to different parent dendrites (**Fig. 4c**). In these cases, the conversion of shaft synapse to spine synapse would require the synchronized elongation of one spine and retraction of another. However, the boutons of asymmetric shaft synapses rarely contained MSBs (1 of 25; **Supplementary Table 2**

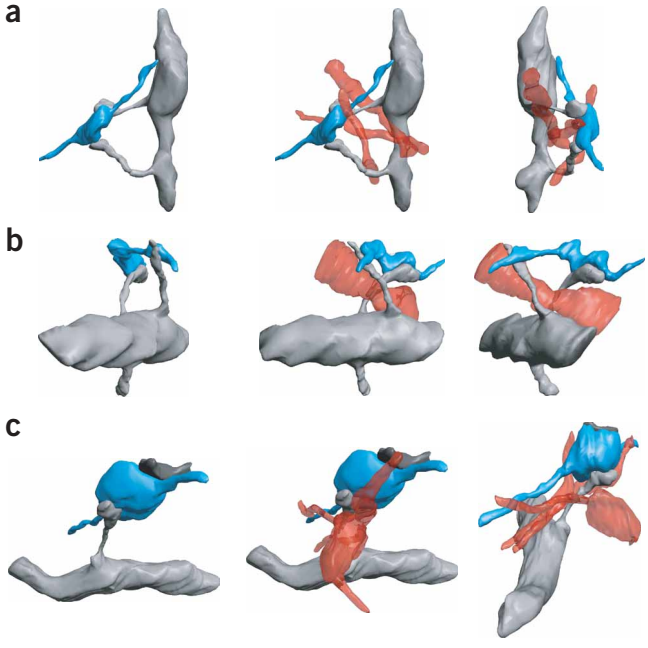

Figure 4 Analysis of the neuropil surrounding imaged spines. (**a**–**c**) Reconstructions of new spines (light gray) and their target axons (blue). Left and middle, same view. Middle column also shows other neurites in the surrounding neuropil (red). Right column, different view of the elements displayed in the middle column. In **a** and **b**, two new spines with the same parent dendrite are making synapses with the same axon. In **c**, a new spine is making a synapse with a bouton that also has a synapse with a second spine (dark gray).

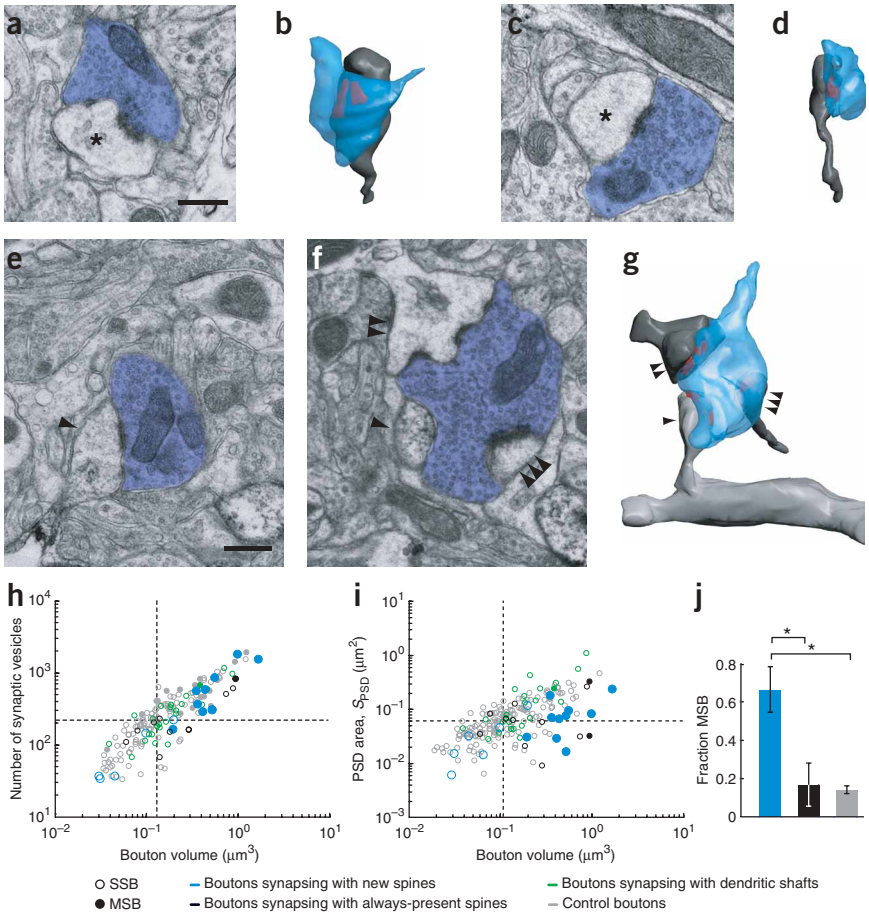

Figure 5 Analysis of synaptic terminals. (**a**–**d**) Electron micrographs (**a**,**c**) and ssEM reconstructions (**b**,**d**) of two control boutons (blue) that make synapses with single dendritic spines (black asterisk). (**e**,**f**) Electron micrographs of a bouton (blue) that has a synapse with a new dendritic spine (single arrowhead in **e**; spine 2 in **Fig. 1**, age 17 d) and two other spines (two and three arrowheads). (**g**) Corresponding ssEM reconstruction. (**h**) The number of synaptic vesicles as a function of the bouton volume. Dashed lines represent the control bouton median values (including MSBs). (**i**) PSD area as a function of the bouton volume. Note that in this plot, the population of control boutons does not include MSBs. (**j**) The fraction of boutons with more than one synapse (fraction MSB). The error bars (s.e.m.) were computed using the binomial distribution. Scale bars in **a** and **e**, 0.5 μm.

lated ($R = 0.92$; $P < 0.001$; **Fig. 5h**), and both varied over a factor of ~100. Less than half of the boutons (30%) contained mitochondria.

In addition, we measured the number and sizes of the synapses on each bouton by measuring the PSD area on the apposed postsynaptic elements. The number of synapses on the boutons varied from 1 to 3, but overall only a small fraction of boutons showed more than one synapse (14%; **Fig. 5h–j**). These MSBs were larger than single-synapse boutons (SSBs) (correlation between bouton volume and synapse number, $R = 0.38$, $P < 0.001$). The boutons contacted by always-present spines were indistinguishable from the control population; they were broadly distributed in volume and vesicle number (**Fig. 5h**) and 17% were MSBs (**Fig. 5j**). Consistent with previous measurements in the hippocampus, PSD area was highly correlated with bouton parameters ($R = 0.80$; $P < 0.001$; **Fig. 5i**). The boutons contacted by new spines had large volumes on average; this was because 67% of them were MSBs that made additional synapses with other spines ($P < 10^{-4}$ compared to control boutons; $P < 0.005$ compared to boutons contacting always-present spines; **Fig. 5h–j** and **Supplementary Table 1**). Our data implies that new spines preferentially make synapses with existing boutons, resulting in MSBs. However, the SSBs contacted by new spines were morphologically similar to control boutons (**Fig. 5h,i**), suggesting that the formation of morphologically mature boutons is coincident with synapse formation.

DISCUSSION

To investigate the relationship between spine addition and synapse formation, we combined high-resolution *in vivo* imaging with electron microscopy. We reconstructed new and always-present spines and other synapses in their vicinity. New spines always had synapses if they persisted for a few days or more. They preferentially formed synapses on boutons that also had other synapses. Our data argue for models of spinogenesis in the adult brain in which spines grow toward presynaptic elements to make synapses.

online), arguing against this possibility. The geometries of more than half of new spines with synapses (**Fig. 4**) are thus difficult to reconcile with the Miller-Peters model. In addition, the observation that the youngest spines often lack synapses (**Fig. 2**) also contradicts the Miller-Peters model. Instead, our data suggest that in the adult brain spines grow toward a presynaptic element to form a synapse, and therefore spine growth precedes synapse formation[23].

New spines form synapses on existing boutons

To determine whether synapses on new spines belong to a particular class and whether they can be distinguished from other L1 synapses, we analyzed a control population of boutons in the neuropil in the vicinity of the imaged L5B dendrites. We reconstructed all boutons fully contained in the image stacks around the imaged dendrite that also made asymmetric synapses with dendritic spines (204 control boutons, **Fig. 5a–d**; 14 boutons contacted by 15 new spines, **Fig. 5e–g**; 11 boutons contacted by 12 always-present spines). We measured bouton volumes and estimated the number of synaptic vesicles they contained (Methods). Bouton volumes and vesicle numbers were highly corre-

New persistent spines have synapses

All spines that were observed for two or more imaging sessions, mostly 4 d apart, always displayed synapses. In contrast, approximately three-fourths of the spines that were reconstructed immediately after they were first seen did not have synapses. Given our imaging interval of 4 d, these new spines could be 0–4 d old. However, based on previous time-lapse measurements[14,16], we can calculate the expected mean age of new spines. Daily measurements indicate that new spines typically retract rapidly with an exponential time course[14]. For our data set, new spines disappeared with a time constant of 2.4 d (ref. 16). Assuming a constant rate of spine growth, this implies that most of the spines (67%) seen once were probably less than 2 d old, with a mean age of ~1.5 d (**Supplementary Note** online).

Our data therefore suggest that new spines make synapses over a prolonged time, probably exceeding 1 d. This is in contrast with studies in cultured preparations, which have shown that excitatory synapses might form within 1–2 h after axodendritic contact[29,37]. In these studies, the enrichment of synaptic markers and vesicle cycling was used as a measure of synapse formation. It is possible that our morphological criteria to define synapses are more stringent and may therefore represent synapses in a more advanced state of assembly. In addition, the dynamics of synapse formation could be different in the adult brain *in vivo* compared to developing neurons *in vitro*.

The existence of naked young spines could indicate three distinct biological processes. First, all new spines could make synapses at some point during their life cycle, but, because ssEM represents a single snapshot of each spine's life cycle, the probability of harvesting spines before synapse formation or after synapse elimination could be substantial[31]. Second, although the growth of all new spines might subserve synapse formation, a fraction of spines could fail in forming a synapse before retracting. Third, distinct populations of protrusions might subserve synaptic and nonsynaptic functions. Further experiments with better temporal resolution in combination with molecular markers of synapses are required to distinguish between these possibilities.

Structural maturation of new spines

New spines differed structurally from always-present spines in having a larger surface-to-volume ratio (S_{sp}/V_{sp}). Similarly, new spines without synapses had larger S_{sp}/V_{sp} than those with synapses. Together with quantifications based on *in vivo* time-lapse images, these observations indicate that spines initially grow as thin, filopodia-like protrusions and that they progressively mature into mushroom spines by adding spine head volume (for example, spines 6 and 7 in **Supplementary Fig. 3**; and **Supplementary Fig. 4** online). Furthermore, most always-present spines contained SER or a spine apparatus, whereas only a few of the new spines contained SER, but never a spine apparatus. Of the new spines, only the ones with synapses contained SER. This indicates that spine maturation is accompanied by the occurrence of SER, similar to the changes that have been observed as a function of development age[33,38]. Because the SER is involved in Ca^{2+} clearance and Ca^{2+}-dependent Ca^{2+} release[39], mature spines could experience different forms of Ca^{2+} dynamics compared to new spines.

It is important to point out that structural differences between these different spines were detected only at the level of populations. The distributions of structural parameters overlapped substantially between groups (**Fig. 3c**). At the level of individual spines, structure was a poor predictor of the presence of synapses. Some thin spines without a head were observed to have synapses (for example, spines 3 and 4 in **Fig. 3a**; also refs. 2,10). It is therefore hard to justify grouping dendritic spines into nonsynaptic 'filopodia' and synaptic spines based on structural criteria from optical microscopy[13,15].

Spine growth precedes synapse formation

The exact relationship between spine addition and synapse formation is unclear[22]. In the Miller-Peters model, spine addition converts a shaft synapse to a spine synapse[21]. As spines grow, their synapses and presynaptic axons move away from the parent dendrite through the neuropil. In this model, spine addition is therefore not coupled to synapse formation. Alternatively, in the Filopodia model, spines grow toward axons to make *de novo* synapses[23].

From our combined *in vivo* and ultrastructural analysis, the Miller-Peters model is very unlikely to apply to the situation in the adult brain. First, axons, dendrites and astrocytic processes are very densely packed in the neuropil (**Figs. 1e** and **2a**; **Supplementary Figs. 2** and **3**) and highly entangled (**Fig. 4**). It is difficult to imagine that an axon can move laterally through the neuropil over distances that cross multiple intervening axons and dendrites. Second, because most axons make *en passant* synapses, the Miller-Peters model predicts that axons must have regions of high local curvature and that these curves would change over time as spines grow and retract. However, excitatory axons have locally straight trajectories[40]. Moreover, axonal trajectories remain straight and stable over time[36]. Third, new spines preferentially made synapses on MSBs. These boutons are presumably anchored in the neuropil by one synapse as the second synapse forms. It is possible that the conversion of shaft synapse to spine synapse involves the synchronized elongation of one spine and retraction of another. However, we found that shaft synapses are rarely associated with MSBs, arguing against this possibility. Fourth, in two cases, we observed two new spines making synapses with the same axon. The two new spines, their parent dendrite and target axon enclosed numerous axons and dendrites. Conversion of a shaft synapse to a spine synapse would require the target axon to cross other neurites or to undergo dramatic and convoluted shape changes. Fifth, the youngest spines often lacked synapses (**Fig. 2**; **Supplementary Figs. 2** and **3**), suggesting that spine growth precedes synapse formation. Our data are therefore largely incompatible with the Miller-Peters model, and consistent with synapse formation by spinogenesis in the adult brain[23]. It remains to be determined whether the Miller-Peters model of spinogenesis operates during development[20].

Is spine loss associated with synapse elimination? Synapse densities in the adult brain are either stable or decrease with age[41]. Our finding of synapse formation in the adult brain therefore argues that synapse elimination is also likely to occur. In addition, a previous study analyzed dendritic segments where spines had retracted[10] and found that the number of shaft synapses on these dendrites could not account for the number of lost spines, arguing that synapse elimination had occurred.

New spines preferentially synapse onto existing boutons

Synapse formation by new spines could be associated with the induction of new boutons (**Supplementary Fig. 4**). Alternatively, new spines could preferentially grow toward existing boutons in the neuropil (**Supplementary Fig. 4**). We found that a high proportion of the boutons contacted by new spines were MSBs rather than SSBs. This finding implies that new spines preferentially grow to make synapses with existing boutons[12,42]. However, our data also suggest that some synapse formation involves new boutons. For example, when two new spines contact the same bouton (**Fig. 4b**), one of these spines could have formed a synapse first, probably together with bouton formation, whereas the second spine formed a synapse on an existing bouton.

Assuming that our sample of new spines with synapses is representative of the situation immediately after synapse formation, our data imply that approximately two-thirds of the new spines make synapses on existing boutons, whereas the rest make synapses on new boutons. These numbers are consistent with the rates of turnover of axonal boutons and dendritic spines seen in time-lapse imaging experiments *in vivo*. The fractional turnover of dendritic spines is typically higher than that of *en passant* boutons[14,36], as expected if spines frequently make synapses on existing boutons.

MSBs are relatively rare in the L1 neuropil ($\sim$14%), similar to the situation in other cortical layers[40] and the CA1 of the hippocampus[43]. Does the finding of preferential synapse formation on existing boutons imply that the incidence of MSBs increases with developmental age? We favor the hypothesis that the formation of synapses on MSBs initiates competition between synapses sharing the same bouton. One of the synapses could be pruned with time (**Supplementary Fig. 4**). This type of synaptic competition could be detected by measuring the fraction of

MSBs contacted by new spines as a function of spine age. Another possibility is that new spines selectively make synapses on axons that are characterized by a high incidence of MSBs, such as thalamocortical boutons[44].

Impact on cortical circuits

What changes in circuits underlie memory storage? The synaptic 'weight' is the total synaptic strength between a pair of pre- and postsynaptic neurons, $\sum_{i=1}^{k} q_i$, where k is the number of synapses connecting the neurons and q_i is the strength of synapse i. Experience-dependent weight changes between previously connected neurons could involve modifications of existing synapses[45] or formation and elimination of synapses between previously connected neurons[7]. In this case, because only weight changes are affected, the network's wiring diagram is left unchanged. However, learning might also involve alterations to the wiring diagram, whereby previously unconnected neurons become connected and vice versa. Unlike just changing weights, wiring changes require synapse formation and elimination. Distinguishing between weight changes and wiring changes in general requires EM-level analysis at the level of entire axonal and dendritic arbors and may have to wait for the development of high-throughput serial EM methods[46]. However, our data provide evidence that spine addition with synapse formation can be involved in weight changes. This is demonstrated by the finding that more than one spine on the same dendritic branch sometimes make synapses with the same axon (**Fig. 4**). In these situations, one of the new spines changed the synaptic weight between previously connected neurons.

Physiological measurements in brain slices have shown that coactive synaptic inputs on the same dendritic branch can have a much larger effect on postsynaptic excitation than when inputs of the same strength are distributed over multiple branches[47]. Synapse addition between axons and individual dendritic branches that are already connected, as we have observed (**Fig. 4**), could therefore have a substantial impact on the flow of excitation in cortical networks.

Changes in synaptic connectivity through the growth and retraction of dendritic spines could contribute to information storage in the brain. The maximum information storage capacity due to spine remodeling depends on the number of synaptic circuits achievable by spine growth and retraction[8]. This number has been estimated as $-N_p\,[\,(1-f)\log_2(1-f)+f\log_2 f\,]$ (bits), where N_p is the number of potential synapses. A potential synapse is defined as a region in the neuropil where axon and dendrite are sufficiently close, within a spine length, to make a synapse by spine growth. f is the filling fraction, defined as the ratio of actual and potential synapses. These calculations have assumed that spines can grow to make synapses with equal probability anywhere on the axon. However, we found that spines preferentially grow toward existing boutons (**Fig. 5j**). This indicates that the spacing between boutons, which can be large compared to spine length[40], is an important parameter. Previous studies therefore probably overestimated N_p and the information storage capacity due to spine growth.

In this study, we reconstructed dendrites exclusively from mice that had undergone whisker trimming for 20 d, which drives changes in cortical circuits[48] and modulates the rates of spine growth and retraction with synapse formation and elimination[10,15,16]. *In vivo* imaging experiments indicate that similar types of plasticity also probably occur under baseline conditions, presumably in response to normal ongoing experience[14–16].

METHODS

Imaging. The procedures for *in vivo* imaging have been described[10,14]. Briefly, adult male transgenic mice expressing GFP (line M, ref. 24; age at first imaging session, 2.3–5 months) were used for this study. An optical chamber was constructed over barrel cortex. Apical dendrites of pyramidal neurons in L5B and L2/3 (1 per mouse) were imaged over a period of at least 28 d (for details see ref. 16). Imaged dendrites were second and higher-order branches, located within 100 μm from the surface of the brain and therefore in L1.

Immunocytochemistry. A detailed description of this procedure is given in **Supplementary Methods** online. Immediately after the final imaging session, the anesthesized mice were transcardially perfused with fixative. Then 60-μm sections were cut tangentially to the barrel cortex, parallel to the imaging window. After washing and crypoprotection, sections were freeze-thawed in liquid nitrogen, then incubated overnight in primary antibody (GFP, Chemicon). The following day, they were then incubated in biotinylated secondary antibody, followed by avidin biotin peroxidase complex (ABC Elite, Vector Laboratories). This labeling was revealed with DAB and hydrogen peroxide. Sections were then further stained with osmium tetroxide and uranyl acetate, dehydrated, and embedded in Durcapan resin (Fluka).

ssEM and morphometric analysis. Once the imaged dendrite had been located in the resin-embedded section, serial sections (600–1,000) were cut at 60-nm thickness and collected onto pioloform membrane on single-slot grids. Serial images of the labeled structures were then collected with a digital camera (MegaView III, SIS) inside a Phillips CM12 transmission electron microscope, at a filament voltage of 80 kV. The labeled dendrite, including all of its spines, was subsequently reconstructed in 3D (**Supplementary Fig. 1**) from the serial EM images.

Serial micrographs were aligned using Photoshop software (Adobe), and measurements made using the Neurolucida software (Microbrightfield). These measurements included dendritic spine volume and surface area, as well as PSD surface area. We also analyzed the boutons synapsing with the imaged spines, as well as others unconnected with the dendrite but contained in the same stacks of serial images. All the boutons in the stacks that made at least one asymmetric synapse with a dendritic spine were measured. In addition, we estimated the number of vesicles in these boutons. A vesicle was counted if at least 75% of the membrane that delineated its spherical appearance was visible and a clear center could be seen. Vesicles were counted in every image in which the bouton could be identified.

The immunocytochemistry procedure did not completely fill the structures with DAB reaction product. Instead, the dendrites often contained clustered black aggregates of the labeling as well as smaller grains with a cloudy appearance. In many cases this enabled us to see the cytoplasm in the spines and to score whether they contained SER or spine apparatus. However, because the labeling procedure does not optimally preserve the membranes, it was difficult to distinguish the exact form and size of these membranes (**Fig. 1c**).

Statistics. We used nonparametric bootstrap methods to compute differences between means and medians, and we report the larger P value. Significance was set at $P = 0.01$. Parameter values in the text are mean ± s.d.

Note: Supplementary information is available on the Nature Neuroscience website.

ACKNOWLEDGMENTS

We thank C. Musetti, V. DePaola and B. Burbach for help with the experiments, and M. Chklovskii, R. Weinberg, R. Weimer and K. Zito for comments on the manuscript. This work was supported by the Swiss National Science Foundation (E.W., No. 310000-108246), the Howard Hughes Medical Institute and the US National Institutes of Health (A.H., K.S. and L.W.).

AUTHOR CONTRIBUTIONS

G.W.K. and A.H. contributed equally to this work. G.W.K., A.H. and K.S. planned the experiments. G.W.K. performed the ssEM. A.H. and L.W. performed the *in vivo* imaging experiments. K.S. built the custom two-photon microscope. K.S. and E.W. contributed reagents, materials and analysis tools, and provided financial support. G.W.K., A.H. and K.S. analyzed the data and wrote the paper. G.W.K., A.H., L.W., E.W. and K.S. discussed the results and commented on the manuscript.

COMPETING INTERESTS STATEMENT

The authors declare that they have no competing financial interests.

Published online at http://www.nature.com/natureneuroscience
Reprints and permissions information is available online at http://npg.nature.com/reprintsandpermissions/

1. Beaulieu, C. & Colonnier, M. A laminar analysis of the number of round-asymmetrical and flat-symmetrical synapses on spines, dendritic trunks, and cell bodies in area 17 of the cat. *J. Comp. Neurol.* **231**, 180–189 (1985).
2. Harris, K.M. & Stevens, J.K. Dendritic spines of CA1 pyramidal cells in the rat hippocampus: serial electron microscopy with reference to their biophysical characteristics. *J. Neurosci.* **9**, 2982–2997 (1989).
3. Nusser, Z. *et al.* Cell type and pathway dependence of synaptic AMPA receptor number and variability in the hippocampus. *Neuron* **21**, 545–559 (1998).
4. Kharazia, V.N. & Weinberg, R.J. Immunogold localization of AMPA and NMDA receptors in somatic sensory cortex of albino rat. *J. Comp. Neurol.* **412**, 292–302 (1999).
5. Takumi, Y., Ramirez-Leon, V., Laake, P., Rinvik, E. & Ottersen, O.P. Different modes of expression of AMPA and NMDA receptors in hippocampal synapses. *Nat. Neurosci.* **2**, 618–624 (1999).
6. Katz, L.C. & Shatz, C.J. Synaptic activity and the construction of cortical circuits. *Science* **274**, 1133–1138 (1996).
7. Chklovskii, D.B., Mel, B.W. & Svoboda, K. Cortical rewiring and information storage. *Nature* **431**, 782–788 (2004).
8. Stepanyants, A., Hof, P.R. & Chklovskii, D.B. Geometry and structural plasticity of synaptic connectivity. *Neuron* **34**, 275–288 (2002).
9. Knott, G.W., Quairiaux, C., Genoud, C. & Welker, E. Formation of dendritic spines with GABAergic synapses induced by whisker stimulation in adult mice. *Neuron* **34**, 265–273 (2002).
10. Trachtenberg, J.T. *et al.* Long-term *in vivo* imaging of experience-dependent synaptic plasticity in adult cortex. *Nature* **420**, 788–794 (2002).
11. Turner, A.M. & Greenough, W.T. Differential rearing effects on rat visual cortex synapses. I. Synaptic and neuronal density and synapses per neuron. *Brain Res.* **329**, 195–203 (1985).
12. Yankova, M., Hart, S.A. & Woolley, C.S. Estrogen increases synaptic connectivity between single presynaptic inputs and multiple postsynaptic CA1 pyramidal cells: a serial electron-microscopic study. *Proc. Natl. Acad. Sci. USA* **98**, 3525–3530 (2001).
13. Grutzendler, J., Kasthuri, N. & Gan, W.B. Long-term dendritic spine stability in the adult cortex. *Nature* **420**, 812–816 (2002).
14. Holtmaat, A.J. *et al.* Transient and persistent dendritic spines in the neocortex *in vivo*. *Neuron* **45**, 279–291 (2005).
15. Zuo, Y., Yang, G., Kwon, E. & Gan, W.B. Long-term sensory deprivation prevents dendritic spine loss in primary somatosensory cortex. *Nature* **436**, 261–265 (2005).
16. Holtmaat, A., Wilbrecht, L., Knott, G.W., Welker, E. & Svoboda, K. Experience-dependent and cell-type-specific spine growth in the neocortex. *Nature* **441**, 979–983 (2006).
17. Engert, F. & Bonhoeffer, T. Dendritic spine changes associated with hippocampal long-term synaptic plasticity. *Nature* **399**, 66–70 (1999).
18. Maletic-Savatic, M., Malinow, R. & Svoboda, K. Rapid dendritic morphogenesis in CA1 hippocampal dendrites induced by synaptic activity. *Science* **283**, 1923–1927 (1999).
19. Toni, N., Buchs, P.A., Nikonenko, I., Bron, C.R. & Muller, D. LT*P* promotes formation of multiple spine synapses between a single axon terminal and a dendrite. *Nature* **402**, 421–425 (1999).
20. Harris, K.M. Structure, development, and plasticity of dendritic spines. *Curr. Opin. Neurobiol.* **9**, 343–348 (1999).
21. Miller, M. & Peters, A. Maturation of rat visual cortex. II. A combined Golgi-electron microscope study of pyramidal neurons. *J. Comp. Neurol.* **203**, 555–573 (1981).
22. Yuste, R. & Bonhoeffer, T. Genesis of dendritic spines: insights from ultrastructural and imaging studies. *Nat. Rev. Neurosci.* **5**, 24–34 (2004).
23. Ziv, N.E. & Smith, S.J. Evidence for a role of dendritic filopodia in synaptogenesis and spine formation. *Neuron* **17**, 91–102 (1996).
24. Feng, G. *et al.* Imaging neuronal subsets in transgenic mice expressing multiple spectral variants of GFP. *Neuron* **28**, 41–51 (2000).
25. Denk, W., Strickler, J.H. & Webb, W.W. Two-photon laser scanning microscopy. *Science* **248**, 73–76 (1990).
26. Vaughan, D.W. & Peters, A. A three dimensional study of layer I of the rat parietal cortex. *J. Comp. Neurol.* **149**, 355–370 (1973).
27. Adams, I. & Jones, D.G. Quantitative ultrastructural changes in rat cortical synapses during early-, mid- and late-adulthood. *Brain Res.* **239**, 349–363 (1982).
28. Colonnier, M. Synaptic patterns on different cell types in the different laminae of the cat visual cortex. An electron microscope study. *Brain Res.* **9**, 268–287 (1968).
29. Okabe, S., Miwa, A. & Okado, H. Spine formation and correlated assembly of presynaptic and postsynaptic molecules. *J. Neurosci.* **21**, 6105–6114 (2001).
30. Peters, A. & Kaiserman-Abramof, I.R. The small pyramidal neuron of the rat cerebral cortex. The perikaryon, dendrites and spines. *Am. J. Anat.* **127**, 321–355 (1970).
31. Petrak, L.J., Harris, K.M. & Kirov, S.A. Synaptogenesis on mature hippocampal dendrites occurs via filopodia and immature spines during blocked synaptic transmission. *J. Comp. Neurol.* **484**, 183–190 (2005).
32. Peters, A., Palay, S.L. & Webster, H.D. *The Fine Structure of the Nervous System.* (Oxford Univ. Press, New York, 1991).
33. Spacek, J. & Harris, K.M. Three-dimensional organization of smooth endoplasmic reticulum in hippocampal CA1 dendrites and dendritic spines of the immature and mature rat. *J. Neurosci.* **17**, 190–203 (1997).
34. Mizrahi, A. & Katz, L.C. Dendritic stability in the adult olfactory bulb. *Nat. Neurosci.* **6**, 1201–1207 (2003).
35. Lee, W.C. *et al.* Dynamic remodeling of dendritic arbors in GABAergic interneurons of adult visual cortex. *PLoSBiol.* **4**, e29 (2006).
36. De Paola, V. *et al.* Cell type-specific structural plasticity of axonal branches and boutons in the adult neocortex. *Neuron* **49**, 861–875 (2006).
37. Friedman, H.V., Bresler, T., Garner, C.C. & Ziv, N.E. Assembly of new individual excitatory synapses: time course and temporal order of synaptic molecule recruitment. *Neuron* **27**, 57–69 (2000).
38. Harris, K.M., Jensen, F.E. & Tsao, B. Three-dimensional structure of dendritic spines and synapses in rat hippocampus (CA1) at postnatal day 15 and adult ages: implications for the maturation of synaptic physiology and long-term potentiation. *J. Neurosci.* **12**, 2685–2705 (1992).
39. Pozzan, T., Rizzuto, R., Volpe, P. & Meldolesi, J. Molecular and cellular physiology of intracellular calcium stores. *Physiol. Rev.* **74**, 595–636 (1994).
40. Braitenberg, V. & Schutz, A. *Anatomy of the Cortex* (Springer Verlag, Berlin, 1991).
41. Micheva, K.D. & Beaulieu, C. Quantitative aspects of synaptogenesis in the rat barrel field cortex with special reference to GABA circuitry. *J. Comp. Neurol.* **373**, 340–354 (1996).
42. Jones, T.A., Klintsova, A.Y., Kilman, V.L., Sirevaag, A.M. & Greenough, W.T. Induction of multiple synapses by experience in the visual cortex of adult rats. *Neurobiol. Learn. Mem.* **68**, 13–20 (1997).
43. Shepherd, G.M. & Harris, K.M. Three-dimensional structure and composition of CA3–CA1 axons in rat hippocampal slices: implications for presynaptic connectivity and compartmentalization. *J. Neurosci.* **18**, 8300–8310 (1998).
44. Lu, S.M. & Lin, R.C.S. Thalamic afferents of the rat barrel cortex: a light- and electron-microscopic study using Phaseolus vulgaris leucoagglutinin as an anterograde tracer. *Somatosens. Mot. Res.* **10**, 1–16 (1993).
45. Malinow, R. & Malenka, R.C. AMPA receptor trafficking and synaptic plasticity. *Annu. Rev. Neurosci.* **25**, 103–126 (2002).
46. Denk, W. & Horstmann, H. Serial block-face scanning electron microscopy (SBFSEM) to reconstruct 3D tissue nanostructure. *PLoSBiol.* **2**, e329 (2004).
47. Polsky, A., Mel, B.W. & Schiller, J. Computational subunits in thin dendrites of pyramidal cells. *Nat. Neurosci.* **7**, 621–627 (2004).
48. Fox, K. Anatomical pathways and molecular mechanisms for plasticity in the barrel cortex. *Neuroscience* **111**, 799–814 (2002).